Modeling and simulation of start/stop system for reduction of vehicle fuel consumption and air pollutant emissions

Samuel Filgueira da Silva
Jony Javorski Eckert
Fabrício Leonardo Silva
Ludmila Corrêa de Alkmin e Silva
Franco Giuseppe Dedini
University of Campinas - UNICAMP

ABSTRACT

In the last decades, energy-efficient road transportation has become one of the major concerns of many countries worldwide. Governmental regulation standards are progressively strict with respect to the maximization of vehicle fuel economy as well as the mitigation of tailpipe emissions. In this scenario, the automotive industry has been providing potential alternatives to address this current issue. One of those possible solutions is the start/stop (SS) system, which consists of an engine shutdown strategy that prevents idling operation. Vehicle idling results in a relevant fraction of fuel consumption and air pollutant emissions, especially in urban driving conditions. Therefore, this study aims to simulate a SS system in an internal combustion engine vehicle model in order to evaluate its improvements in fuel consumption and reduction of generated tailpipe gases. The vehicle simulation model is developed in Matlab/Simulink™ environment and the exhaust emissions are quantified by the ADVISOR™ fuel converter block. For a further analysis that takes into account different driving conditions, the vehicle will be analyzed under the FTP-75 driving cycle used in emission evaluation procedure and also under a real-world driving cycle.

Keywords: Start/stop system, fuel consumption, exhaust emissions, ADVISOR, vehicle idling

INTRODUCTION

Air quality improvement policies have increasingly become a trend worldwide due to the hazardous effects air pollution has caused to human health and environment. In the Paris agreement [1], [2], many countries (including Brazil) have committed to implement several measures for the reduction of their high gas emission indexes. Furthermore, energy security is another important goal established by authorities through demanding governmental regulations that are able to generate more sustainable cities.

In this scenario, automotive industry plays an important role to address such concern as internal combustion engine vehicles contribute significantly to the urban air pollution and consequent environmental impacts [3], [4] and require a huge amount of fossil fuel resources [5], which are predicted to be considerably lower in about two decades if the oil consumption still follows the current rate [6], [7]. Miao et al. [8] present a study case of gas emissions in China and explain that nitrogen oxides (NO_x) are of major concern due to the fact that they are one of the most dangerous gases for large amounts constantly released in the atmosphere. In their work, they show that the road transportation activity is one of the main contributors to the emission of such toxic gas. Besides, several studies have presented that motor vehicle emissions are directly associated to different ecosystem and people's health damages [9]–[11].

Thus, researchers have extensively discussed about innovative systems and vehicle-based modifications that can provide low-emission and fuel-efficient vehicles. Such alternatives include vehicle redesign with lighter-weight materials [12], devices for aerodynamic drag reduction [13], tire design to decrease rolling resistance [14], [15], drivetrain design improvement [16], [17] and engine downsizing [18]. Moreover, studies have shown that an optimum gear shifting control results in significant reduction of gas emissions and vehicle fuel consumption [19]–[21]. Hybridization is another appealing alternative to achieve better fuel economy and emission indexes [22], [23].

One of those attractive solutions with reasonable price is the start/stop (SS) system, which can mitigate exhaust emissions as well as fuel consumption by switching off the engine automatically when no propulsion is requested by the driver. Since the engine idling condition consists of a relevant amount of fuel consumed and air pollutant emissions [24], SS technology, which prevents such idle periods, has increasingly been used in automotive manufactures such as Nissan [25], Ford [26], General Motors [27], BMW [28], and others.

Previous works have proposed SS strategies for hybrid vehicles in order to increase mileage and reduce gas emissions [29], [30]. For their SS controllers, different input parameters are considered (e.g. required torque, vehicle speed, battery state-of-charge etc.) and the engine is turned off as long as the driving conditions meet all the SS strategy constraints. Furthermore, Bishop et al. [31] implement a belt-driven starter/alternator into a GMC Envoy to assist the start/stop management of its 4.2L six-cylinder engine. Their study obtains the fuel consumption reduction of 5.3% and 4.0% in urban and highway driving cycles, respectively. Wishart et al. [32] carry out dynamometer and fleet tests to evaluate the benefits of the implementation of idle-stop (IS) systems in passenger vehicles for different driving cycles, achieving the fuel economy improvement of 6.3% (NEDC cycle) and 7.1% (JC08 cycle) for the Volkswagen Golf as well as 8.3% (NEDC cycle) and 7.0% (JC08 cycle) for the Mazda 3. With respect to greenhouse gases, Fonseca et al. [33] present a substantial decrease of such emissions with the integration of SS technology on a four-wheel-drive diesel vehicle. In another approach, scientists have investigated the effective idle stop or break-even point [28], [34]–[37], that is, the minimum time the engine has to be switched off to generate higher fuel saving than the energy needed to restart the engine. In published literature, it is possible to infer that idle time of less than 3 s usually results in ineffective engine stop [28].

In this paper, a SS system is simulated for a conventional vehicle equipped with 1.0L 4-cyclinder gasoline engine. The vehicle model runs under the urban FTP-75 and real-world (Campinas city) driving cycles so that fuel consumption and air pollutant emission indexes' improvements can be evaluated. Such exhaust emissions are measured according to the ADVISOR™ fuel converter block and the model is simulated in Matlab/Simulink™ environment.

LONGITUDINAL VEHICLE DYNAMICS

In this paper, the longitudinal vehicle modeling is introduced according to the governing equations, as proposed by Gillespie [38]. In addition, the maximum tire-ground and clutch transmissible torque constraints [19] are incorporated in the vehicle model. Figure 1 illustrates the resistive forces the vehicle is subject to during motion.

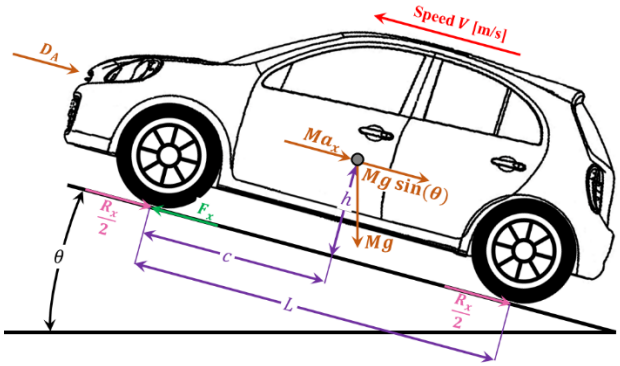

Figure 1 – Free-body diagram of vehicle adapted from [21]

The required torque T_{rw} [Nm] can be calculated by Equation 1, as a function of tire dynamic radius r [m], the inertia force (vehicle mass M [kg] and required acceleration a_{req} [m/s^2]), rolling resistance R_x [N], aerodynamic drag D_A [N] and climbing resistance (vehicle weight W [N] and road angle θ [º]). The latter is only considered in the model running on the real-world driving cycle based on Campinas city. For the standard FTP-75 drive cycle, the gravitational force is not taken into account as the road grade is assumed as null.

$$T_{rw} = \left(Ma_{req} + R_x + D_A + Wsin(\theta)\right)r \quad (1)$$

The aerodynamic drag D_A [N] is due to the wind resistance and opposes to the vehicle motion. Such resistive force is dependent upon vehicle body geometry and air properties and can be determined by Equation 2, where ρ [kg/m^3], C_d and A [m^2] are the air density, drag coefficient and frontal area of the vehicle, respectively. Besides, D_A varies directly as the square of the vehicle speed V [m/s].

$$D_A = 0.5\rho V^2 C_d A \quad (2)$$

The rolling resistance R_x [N], on the other hand, is given by the energy loss generated by road-tire interface. This load is of great importance at low speeds and can be expressed by Equation 3.

$$\mathrm{R_x} = 0.01\left(1 + \frac{2.24\mathrm{V}}{100}\right)\mathrm{W} \quad (3)$$

With respect to the dynamic radius r, it is defined as a function of the geometric radius r_g and the correction factor k_v, which is influenced by the vehicle speed.

$$r = 0.98r_g(1 + 0.01k_v) \quad (4)$$

The speed profile provided by the analyzed driving cycles (FTP-75 and Campinas city) is the target speed. The required acceleration for the model is then calculated according to the difference between the desired speed V_d at the next time step $(t + \Delta t)$ and actual speed V at the current simulation time t, divided by the time step Δt itself, as shown in Equation 5.

$$a_{req}(\mathrm{t}) = \frac{\mathrm{V_t}(\mathrm{t} + \Delta t) - V(t)}{\Delta t} \quad (5)$$

Once determined the required torque for the vehicle model, it is possible to calculate the respective engine required torque T_{ICE} [Nm], expressed by Equation 6, as a function of the engine inertia I_e [kgm^2], gearbox inertia I_t [kgm^2], differential inertia I_d [kgm^2], wheels and tires' inertia I_w [kgm^2], differential gear ratio N_d, transmission gear ratio N_t and overall powertrain efficiency η_{td}.

$$T_{ICE} = \frac{T_{rw} + \left((I_e + I_t)(N_t N_d)^2 + I_d {N_d}^2 + I_w\right)\frac{a_{req}}{r}}{N_t N_d \eta_{td}} \quad (6)$$

However, such delivered torque by the engine should be limited to its maximum (wide-open throttle) torque curve, as depicted by Figure 2. For conditions T_{ICE} is greater than the maximum engine torque T_{ICE}^{max} at certain speed, the former is limited by the value of the latter.

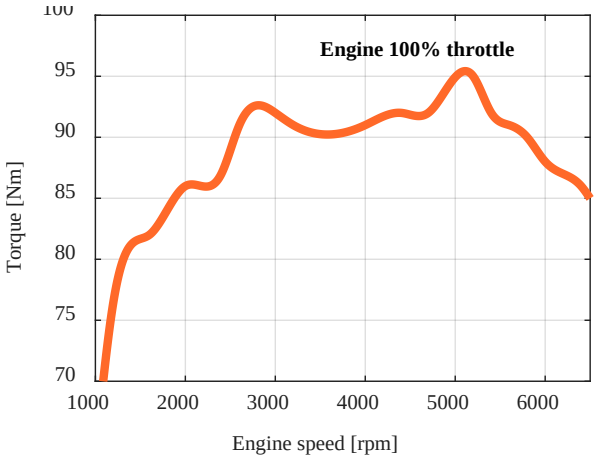

Figure 2 – Wide-open throttle engine torque curve [20], [22]

Furthermore, during the gear shifting, the clutch is another limiting factor for the available gearbox input torque. This happens due to the fact that the engine is not able to deliver the same amount of required torque T_{ICE} since the ICE decouples from the transmission [39]. Thus, the clutch transmissible torque T_{CL} is determined by Equation 7, as proposed by Kulkami, Shim and Zhang [40], according to its friction coefficient μ_{cl}, external R_o and internal R_i disks' radii [m] and number of faces n. For the simulation model, the gear shifting process was introduced based on the procedure defined in [20], [21]. The time of 0.3 s was assumed for the ICE decoupling from the gearbox, followed by the posterior gear shifting during 0.2 s and, finally, the gradual clutch recoupling, which occurs for 0.5 s. The clutch spring force F_n [N] varies according to the pedal position, as presented in Figure 3.

$$T_{CL} = \frac{2}{3}\mu_{cl} F_n n \frac{{R_o}^3 - {R_i}^3}{{R_o}^2 - {R_i}^2} \quad (7)$$

The gearbox input torque T_{gb} is then given by the minimum value among the engine required torque T_{ICE}, maximum engine torque T_{ICE}^{max} and the clutch transmissible torque T_{CL}, as described by Equation 8. The available torque transferred to the wheels, on the other hand, can be calculated by Equation 9, as a function of the parameters described previously.

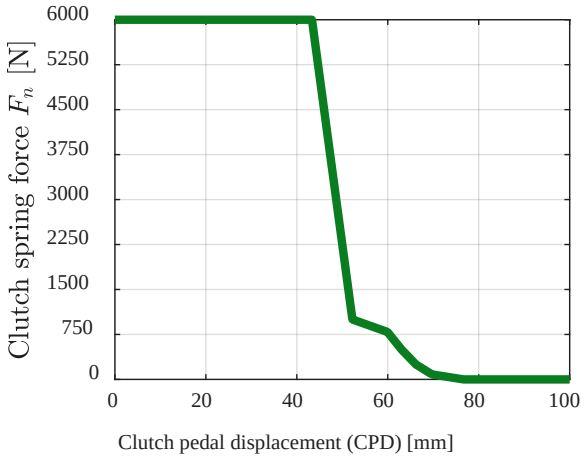

Figure 3 – Clutch spring force behavior along clutch pedal position variation [20], [22]

$$T_{gb} = \min\{T_{ICE}, T_{ICE}^{max}, T_{CL}\} \quad (8)$$

$$T_w^{av} = T_{gb} N_t N_d \eta_{td} - \left((I_e + I_t)(N_t N_d)^2 + I_d {N_d}^2 + I_w\right)\frac{a_{req}}{r} \quad (9)$$

In addition, the tire traction limit is another condition that eventually reduces vehicle performance as a result of tire slipping. To address such issue, in this study, the tire-ground transmissible torque $T_{tg(max)}$ model (Equation 10), as described by [41], is considered as a constraint in the determination of the effective torque delivered to the wheels T_w^{eff}, which can be expressed by Equation 11.

$$T_{f(max)} = \mu\left(\frac{Wc}{2L} - \frac{Wha_x}{2Lg}\right) \quad (10)$$

Where:
L = Wheelbase [m]
h = Height of the vehicle's center of gravity [m]
g = Gravity [m/s^2]
c = Longitudinal distance between the vehicle's rear axle and its gravity center [m]

$$T_w^{eff} = \min\{T_w^{av}, T_{f(max)}\} \quad (11)$$

Due to the limiting factors described previously, the vehicle acceleration a_x, which can be expressed according to Equation 12, may be below the required acceleration a_{req}. In the case that actual vehicle acceleration a_x is inferior to the required one, the simulation carries out an iterative process, among Equations 6 to 12, in such a way that a_{req} is assumed equal to a_x until convergence. As a result of this, the greatest possible acceleration value is defined. Therefore, the effective engine output torque can be determined, as shown in Equation 13.

$$a_x = \frac{\frac{T_w^{eff}}{r} - R_x - D_A - Wsin(\theta)}{M} \quad (12)$$

$$T_{ICE}^{eff} = \frac{T_w^{eff} + \left((I_e + I_t)(N_t N_d)^2 + I_d {N_d}^2 + I_w\right)\frac{a_x}{r}}{N_t N_d \eta_{td}} \quad (13)$$

Finally, the effective engine speed ω_{ICE}^{eff} is given by Equation 14, as a function of the tire slip coefficient e (Figure 4), which varies according to the effective torque T_w^{eff}.

$$\omega_{ICE}^{eff} = \frac{N_d N_t V}{r(1-e)} \quad (14)$$

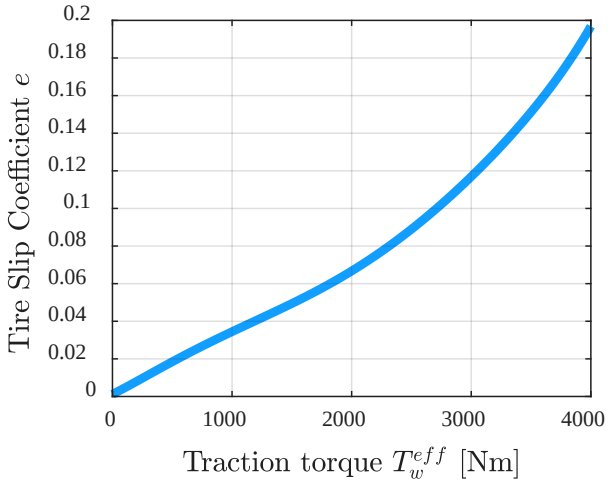

Figure 4 – Tire slip coefficient variation according to the effective traction torque

VEHICLE MODEL

In order to simulate the SS system influence on vehicle fuel consumption and exhaust emissions, a vehicle model is developed in Matlab/Simulink™ environment, added to the fuel converter block from ADVISOR™.

In this study, the model is based on a Brazilian vehicle equipped with a 1.0L 4-cylinder engine. Moreover, the standard gear shifting described in [42] was used as reference for the simulation model presented in this paper. The specification parameters of the vehicle are shown in Table 1.

Table 1 – Vehicle model's parameters

Parameters	Units	Gear				
		1st	2nd	3rd	4th	5th
Engine inertia	kgm^2	0.1367				
Gearbox inertia (x10^{-4})	kgm^2	17	22	29	39	54
Gearbox ratios	-	4.27	2.35	1.48	1.05	0.8
Differential inertia	kgm^2	9.22E-04				
Differential ratio	-	4.87				
Wheels + tires inertia	kgm^2	2				
Vehicle mass	kg	980				
Tires	-	175/70R13				
Clutch external radius	mm	95				
Clutch internal radius	mm	67				
Vehicle frontal area	m^2	1.8				
Drag coefficient	-	0.33				
Wheelbase	m	2.443				
Gravity center height	m	0.53				
Rear axle to gravity center	m	1.46				
Front axle to gravity center	m	0.98				
Tire peak friction coefficient	-	0.9				
Tire radius	m	0.2876				
Clutch friction coefficient	-	0.27				
Clutch faces	-	2				
Vehicle speed	m/s	0	16.67	25	33.33	41.67
k_v factor	-	0	0	0.1	0.2	0.4

ENGINE MODEL

Once the engine operation point is determined according to the equations described previously, the fuel consumed and gas emissions should be determined. In order to do such analysis, this study uses the Advanced Vehicle Simulator (ADVISOR), which is a system-level simulation tool used for the evaluation of fuel consumption and exhaust emissions according to experimental database of vehicles running over standard driving cycles [43]. One of the advantages of ADVISOR™ is that it quantifies the tailpipe emissions taking into account the engine temperature, which influences on catalyst efficiency and, consequently, the results of those emission values [19].

Several works have used this vehicle simulation tool for fuel economy and gas emission analysis [44]–[48]. Thus, in this paper, the unburned hydrocarbons (HC), nitrogen dioxide (NOx) and carbon monoxide (CO) emissions are determined from the ADVISOR™ engine emission maps (shown in Figure 5), so that SS system effectiveness in reducing those indexes can be analyzed.

DRIVING CYCLE

The vehicle model runs on the standard FTP-75 driving cycle (also NBR 6601 [49]), which is included an engine shutdown period to simulate cold and hot start phases, as illustrated by Figure 6.

In order to expand the analysis and compare results for different driving conditions, the simulation is also subject to a real-world driving cycle from Campinas city (shown in Figure 7), where the road altimetry is obtained by data acquisition and used for the determination of the road grade and calculation of the gravitational force acting on the vehicle (Figure 8) [50]. As traffic jam is one of the common issues found in large cities as Campinas, the SS system may be a very interesting alternative to reduce pollutant emissions and fuel consumption in this type of real-world driving scenario.

The driving cycle parameters of both cycles used in this study is presented by Table 2. It is possible to observe that the vehicle idling consists of a relevant fraction of both cycles and, consequently, of fuel consumed and generated tailpipe emissions.

Table 2 – Driving cycles' characteristics

Driving cycle parameters	FTP-75 (NBR 6601)	Real-world (Campinas)
Total distance [km]	17.79	45
Total time [s]	2500	7510
Average speed [km/h]	25.62	20.18
Idling time [%]	39.32	21.52
Maximum speed [km/h]	91.09	73.46

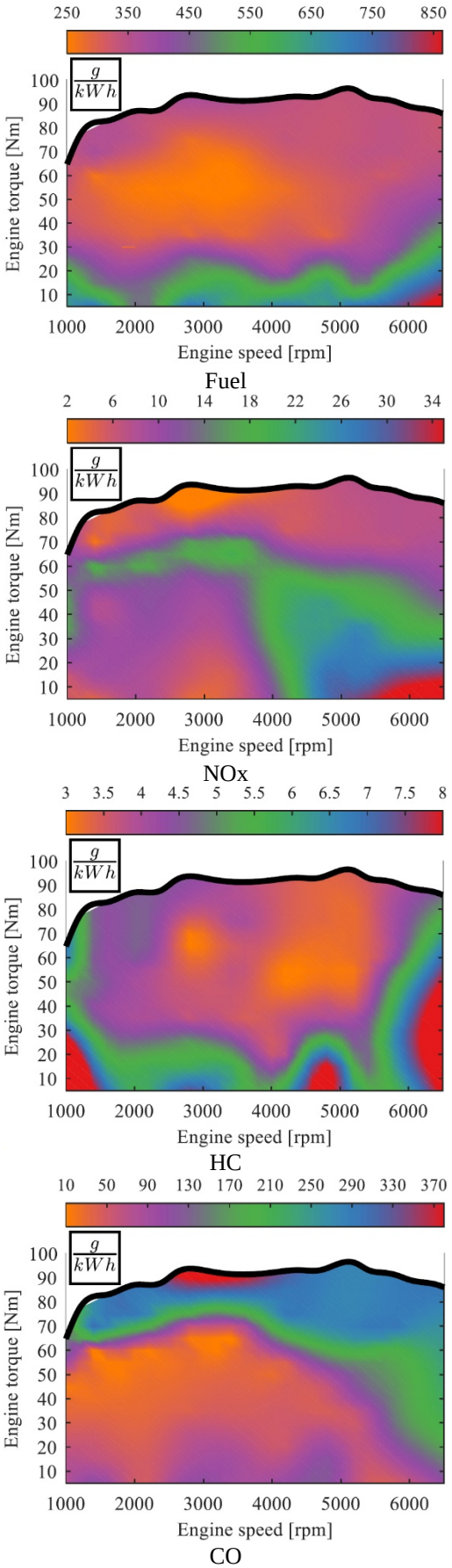

Figure 5 – Engine specific fuel consumption and air pollutant emission maps

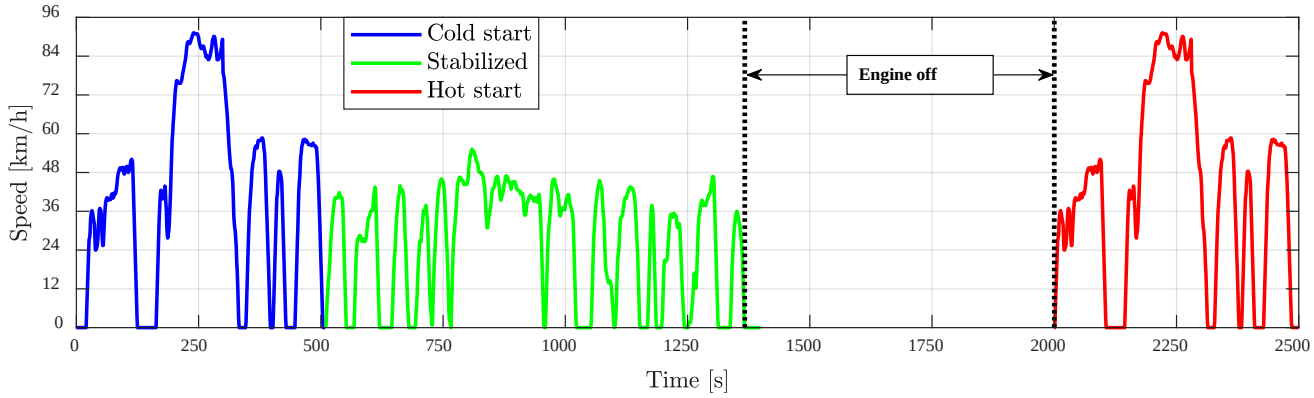

Figure 6 – NBR 6601 cycle. Adapted from [46]

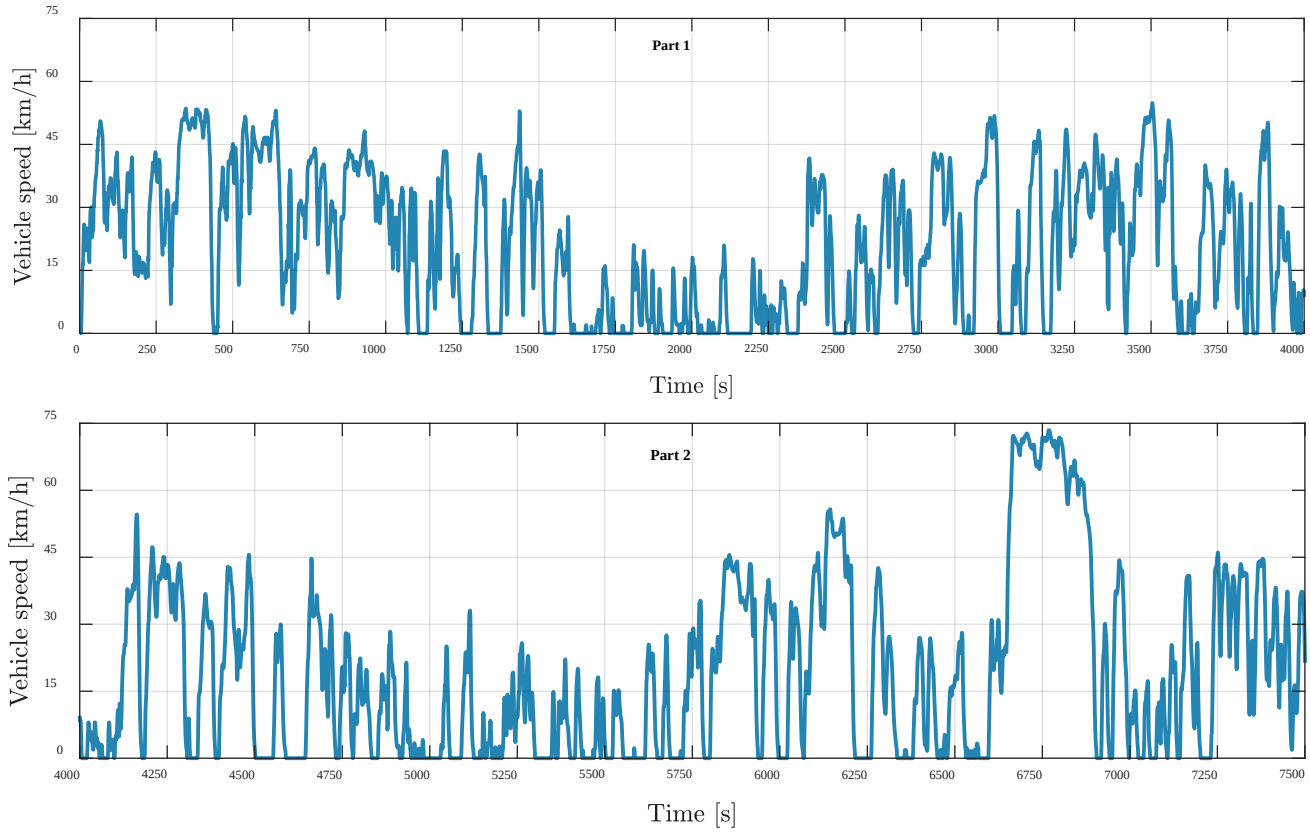

Figure 7 - Campinas driving cycle. Adapted from [46]

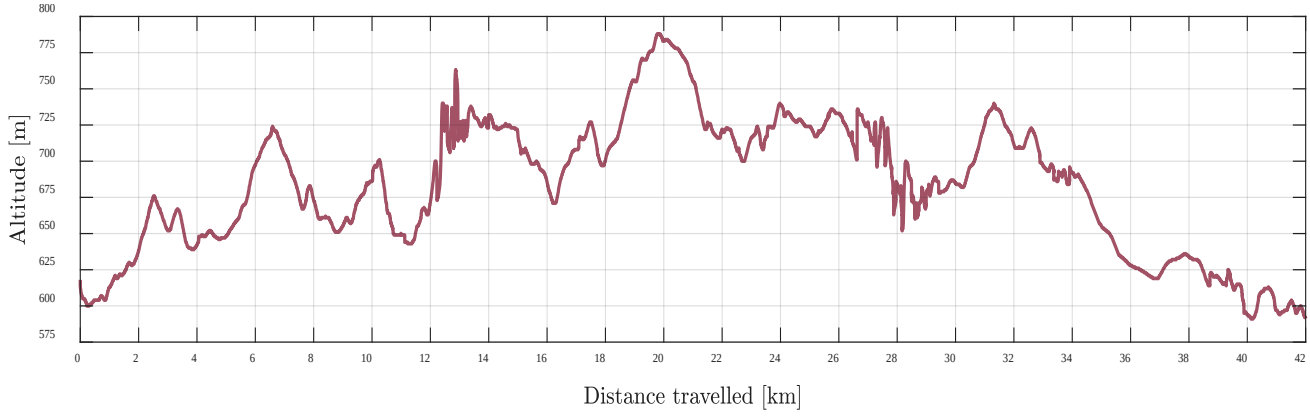

Figure 8 – Altimetry of Campinas driving cycle. Adapted from [46]

START/STOP STRATEGY

With regards to the start/stop simulation model, a strategy that rules the actuation of the system was established, as expressed by Equation 15. The engine temperature C_{ICE} higher than 95 °C was introduced as one of the constraints for the engine shutdown since it avoids the postponement of the engine warmup period, which results in low-efficiency catalyst and, consequently, the increase in gas emissions [19]. The state variable E_{st} is 0 when the engine is switched off and 1 otherwise.

$$E_{st} = \begin{cases} 0, & if: T_{ICE}^{eff} = 0 \text{ and } V = 0 \text{ and } C_{ICE} \geq 95°C \\ 1, & \text{otherwise} \end{cases} \quad (15)$$

In this work, the comparative analysis between the results of fuel economy and tailpipe emissions with and without such engine temperature restriction will be carried out in the following section. Furthermore, the minimum time of engine turned off was set as 7 seconds, which is the effective idle time (break-even point for fuel efficiency), proposed by [36], for a similar engine as the one presented in this study.

SIMULATION RESULTS

The simulation was performed under the urban FTP-75 and Campinas drive cycles, as described previously. It will be evaluated three different conditions, which are the following: the baseline configuration (conventional vehicle); the conventional vehicle model subject to the actuation of the SS system according to the strategy described by Equation 15; and the conventional vehicle subject to SS strategy without engine temperature C_{ICE} constraint.

Since the SS system has more influence on urban traffic conditions that extend the engine warm-up period, the cold-start phase of FTP-75 will be analyzed separately from the rest of the cycle. In a similar approach, the Campinas cycle, which stands for typical real-world driving condition for crowded cities, is also investigated in a specific part of the route. Such condition is characterized by intense traffic jam, where fuel consumption and exhaust emissions are influenced by SS actuation.

FTP-75 DRIVING CYCLE

As the number of engine stops increases during the driving cycle and the engine reaches its steady-state temperature, the SS system starts to achieve more relevant results regarding the reduction of exhaust emissions. Table 3 presents the results of pollutant emissions as well as fuel consumption for all the FTP-75 cycle. It is possible to see that the SS strategy with no C_{ICE} constraint still showed greater amount of emitted CO than baseline configuration. This is due to the fact that the CO emission during engine cold start represents the majority of air pollutants emitted [51]. The SS actuation with engine temperature analysis, on the other hand, achieved 8.92% fuel saving associated with 0.52% CO, 5.66% HC and 2.76% NO_x emissions reduction. Thus, it is possible to infer that such engine-temperature-based SS strategy configuration presented the best performance with respect to the balance between fuel consumption and exhaust emissions.

Regarding the cold-start phase of FTP-75 driving cycle, the baseline configuration results for engine temperature and fuel consumption are depicted by Figure 9. During this engine start condition, it is possible to observe that the engine temperature restriction for the SS strategy development is critical to obtain better results with respect to air pollutant emissions. Despite the fuel economy improvement of 3.59%

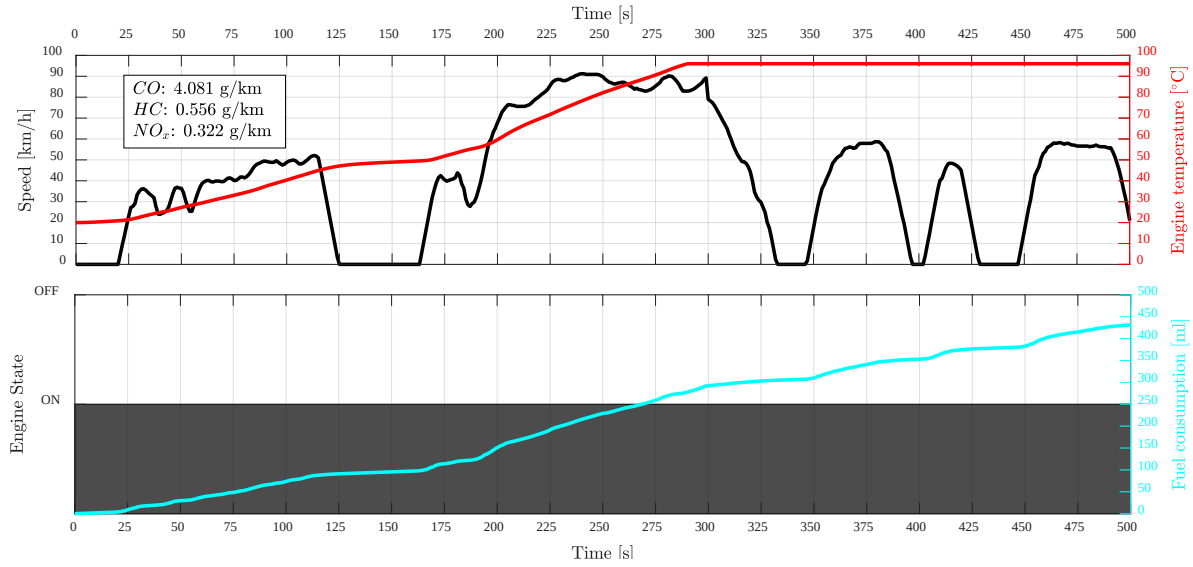

Figure 9 – Engine temperature and fuel consumption for the standard vehicle under cold-start phase of FTP-75 cycle

Table 3 – FTP-75 cycle: emissions and fuel consumption results

Parameters	Conventional	SS	SS with no C_{ICE}
FC [l]	1.456	1.326	1.319
CO [g/km]	1.737	1.728	1.776
HC [g/km]	0.265	0.250	0.246
NO_X [g/km]	0.181	0.176	0.178
Warm-up[s]	287	287	301

generated by SS strategy with no C_{ICE} condition, the CO and NO_x emissions were increased by (3.50% and 1.24%), respectively, when compared to the conventional vehicle equipped with no SS system, as illustrated by Figure 10.

This is due to the extended engine warm-up period [19] (14 s more), which is caused by the higher number of engine shutdowns during the driving profile. Hence, one solution to address this concern is to include a limiting condition that prevents the engine turns off before it reaches its steady-state temperature (95 °C). Furthermore, Figure 11 shows that the all gas emissions' indexes are slightly lower than the conventional vehicle (0.1% CO, 0.36% HC, 0.31% NO_x) when C_{ICE} constraint is introduced since the warm-up time is now the same as the conventional vehicle (287 s). The fuel consumption decreases 1.41% when compared to baseline configuration (425.1 ml against 431.2 ml) and increases 2.21% with regards to the SS strategy with no C_{ICE} condition (425.1 ml against 415.7 ml) as the engine turns off less often.

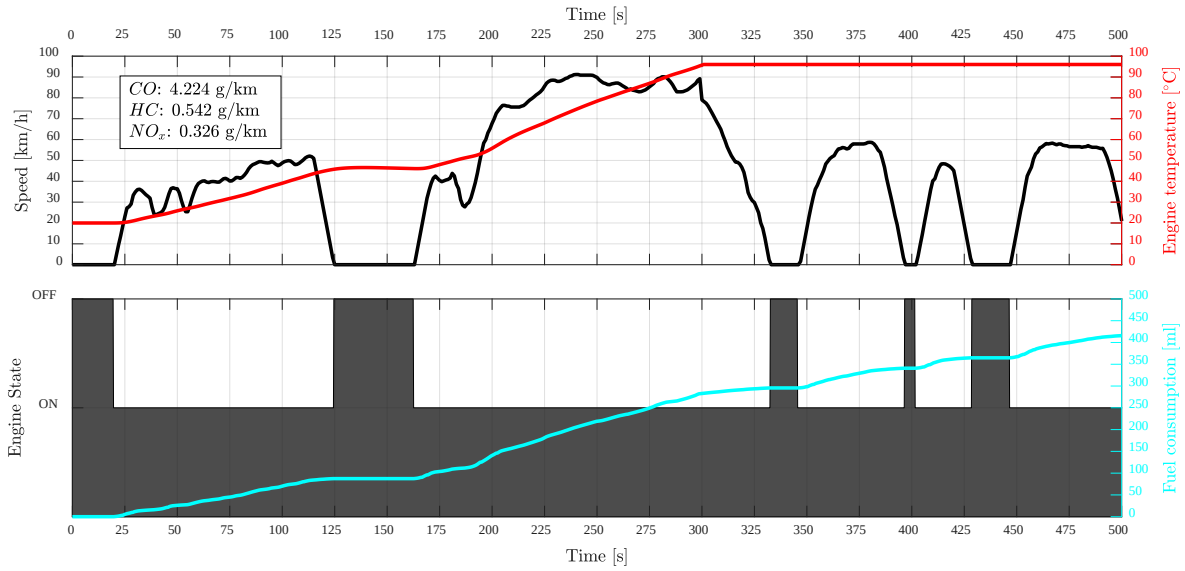

Figure 10 – Engine temperature and fuel consumption: SS system without C_{ICE} restriction under cold-start phase of FTP-75 cycle

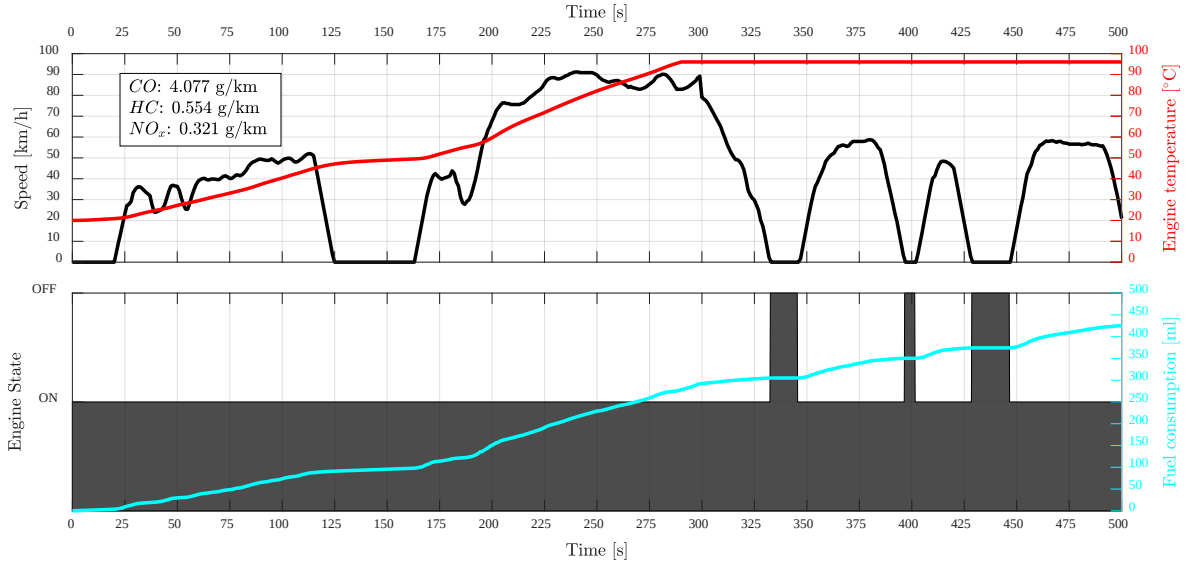

Figure 11 – Engine temperature and fuel consumption: SS system with C_{ICE} restriction under cold-start phase of FTP-75 cycle

CAMPINAS DRIVING CYCLE

In the second analysis, the vehicle model runs under Campinas cycle. This driving condition is different from the urban FTP-75 profile since there is no cold-start phase. In fact, there is only one vehicle stop (the approximate 20 s at the beginning of the cycle) until the engine reaches its steady-state temperature condition. For this reason, the standard vehicle idling occurs in a very short period of time and the engine warm-up time for the three cases analyzed in this paper are very similar to each other, as described by Table 4. Therefore, the SS strategy without C_{ICE} restriction presented lower emission indexes than the baseline configuration for the air pollutants evaluated (-1.19% CO, -3.61% NOx and -6.31% HC), while maximizing the fuel economy in 10.02%. Moreover, the SS system that considers C_{ICE} in its actuation strategy obtained increase of 9.79% in fuel economy as well as a decrease of 1.68% CO, 5.79% HC and 4.22% NO_x emissions.

Table 4 – Campinas cycle: emissions and fuel consumption results

Parameters	Conventional	SS	SS with no C_{ICE}
FC [l]	3.952	3.565	3.556
CO [g/km]	1.010	0.993	0.998
HC [g/km]	0.190	0.179	0.178
NO_X [g/km]	0.166	0.159	0.160
Warm-up[s]	336.4	336.4	337.2

ENGINE START-UP AT TRAFFIC JAM CONDITION

In order to evaluate a possible cold-start phase for the Campinas driving profile, it is assumed that the vehicle starts to run from 1550s onwards as this part of the route consists of a low-speed driving profile (see Figure 7), which results in a long time of engine heating process. In this assumption, the engine starts at ambient temperature (20 °C).

For the three cases analyzed in this study, the engine temperature and fuel consumption curves along 1500 seconds (from 1550 s to 3050 s of the original driving cycle) are presented by Figure 12 (baseline), Figure 13 (SS actuation) and Figure 14 (SS actuation without C_{ICE} restriction). In this driving condition, the vehicle equipped with engine-temperature-based SS strategy achieved the improvement of 1.95% in fuel economy in comparison with the standard configuration, while reducing by 0.34% CO, 1.04% HC and 0.57% NO_x emissions.

However, the SS strategy with no C_{ICE} constraint presented, as in the FTP-75 cold-start phase, higher CO and NO_x emission indexes, that is, an increase of 3.41% and 7.02%, respectively. This is primarily related to the fact that the engine stops prevent its temperature to reach optimal condition (95 °C) quickly. In this case, the engine warm-up is only achieved in 1001 s, while the other configurations showed time of 817 s.

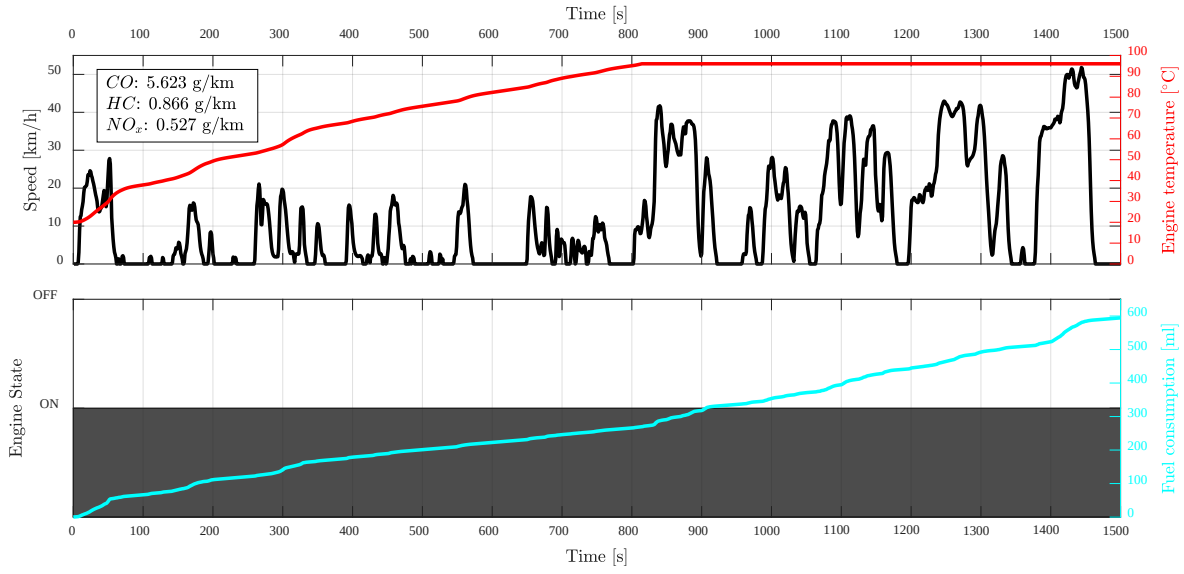

Figure 12 – Engine temperature and fuel consumption for the standard vehicle under hypothetical cold-start phase of Campinas cycle

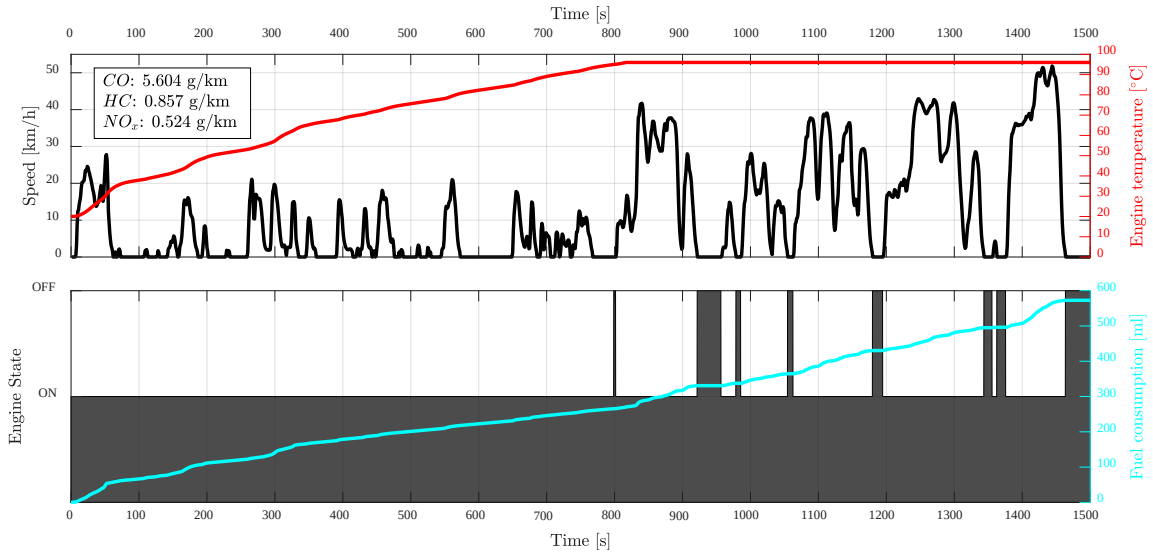

Figure 13 – Engine temperature and fuel consumption for vehicle equipped with SS system with C_{ICE} restriction configuration under hypothetical cold-start phase of Campinas cycle

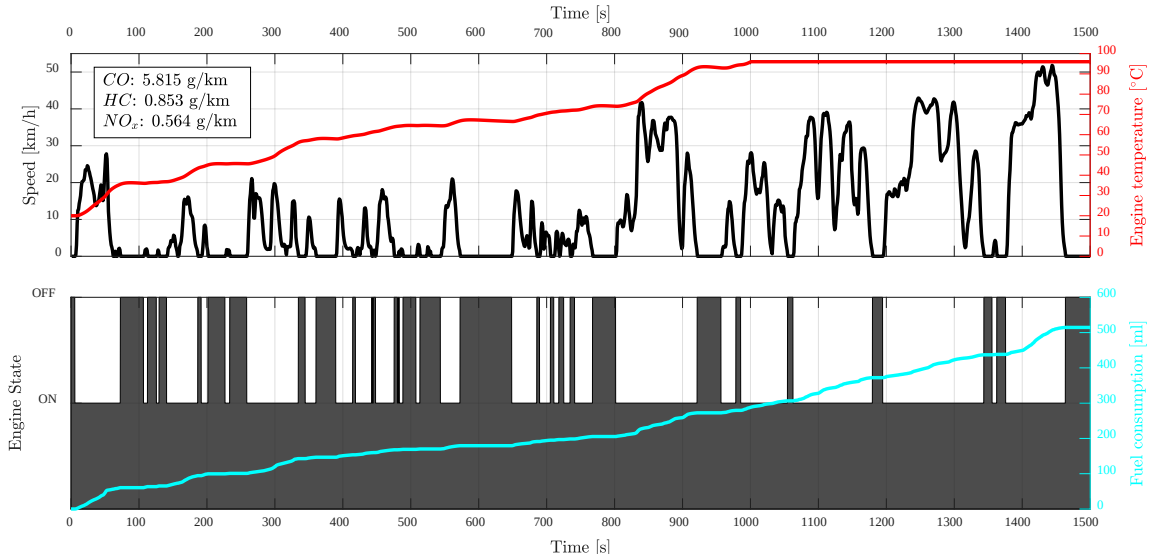

Figure 14 – Engine temperature and fuel consumption for vehicle equipped with SS system without C_{ICE} restriction configuration under hypothetical cold-start phase of Campinas cycle

CONCLUSIONS

In this study, an engine start/stop system was modeled and simulated for a compact vehicle equipped with a 1.0L gasoline engine in order investigate the efficacy of such technology. The vehicle model was developed in MATLAB/Simulink™ environment. The effects of SS system on fuel consumption and air pollutant emissions were evaluated under the FTP-75 (NBR 6601) and Campinas driving cycles using ADVISOR™ simulation tool. Furthermore, the SS strategy was modified by adding the engine temperature constraint, so that the system performance could be analyzed under engine cold start conditions. The SS system presented relevant results with respect to fuel saving in strategy modes with and without engine temperature condition. For engine-temperature-based SS strategy mode, the fuel economy improvement under FTP-75 and Campinas cycle was 8.92% and 9.79%, respectively. The SS with no C_{ICE} constraint, on the other hand, reduced the standard vehicle fuel consumption by 9.40% (FTP-75) and 10.02% (Campinas cycle). Despite the better results with regards to fuel consumption, the SS-without-engine-temperature-restriction strategy mode showed performance issues related to its extended engine warm-up period as the vehicle runs on engine cold-start driving profiles, very common in traffic jam conditions. That resulted in low catalyst efficiency and, consequently, greater CO and NO_x emissions. Therefore, the engine temperature proved to be an important parameter in the SS strategy development since the system can evaluate a more suitable moment to switch off the engine, balancing both fuel saving and tailpipe emissions. Finally, it can be concluded that

start/stop technology can be effective and the engine temperature is an important parameter to consider in the development of its strategy as it directly influences gas emissions. Its low cost and easy integration into vehicle system architecture is found be a good alternative to provide greener and fuel-efficient vehicles, so pursued by modern governmental regulations worldwide. For future works, vehicle tests will be important to validate the simulation model, analyzing the real performance of the SS system.

ACKNOWLEDGEMENT

This work was conducted during scholarships supported by the Brazilian Federal Agency for Support and Evaluation of Graduate Education (CAPES) and the University of Campinas (UNICAMP).

REFERENCES

[1] M. Mace, "Mitigation Commitments under the Paris Agreement and the Way Forward," *Clim. Law*, vol. 6, pp. 21–39, Jan. 2016.

[2] C. A. Horowitz, "Paris Agreement," *International Legal Materials*, vol. 55, no. 4, pp. 740–755, 2016.

[3] R. Smit, P. Kingston, D. W. Neale, M. K. Brown, B. Verran, and T. Nolan, "Monitoring on-road air quality and measuring vehicle emissions with remote sensing in an urban area," *Atmospheric Environment*, vol. 218, p. 116978, 2019.

[4] A. Faiz, "Automotive emissions in developing countries-relative implications for global warming, acidification and urban air quality," *Transportation Research Part A: Policy and Practice*, vol. 27, no. 3, pp. 167–186, 1993.

[5] M. Ehsani, Y. Gao, and A. Emadi, *Modern Electric, Hybrid Electric, and Fuel Cell Vehicles.*, 3rd Editio. Boca Raton: CRC Press, 2018.

[6] M. Abolhassani *et al.*, *Impact of Hybrid Electric Vehicles on the World's Petroleum Consumption and Supply*. 2003.

[7] R. G. Miller and S. R. Sorrell, "The future of oil supply," *Philosophical Transactions of the Royal Society A: Mathematical, Physical and Engineering Sciences*, vol. 372, no. 2006, p. 20130179, Jan. 2014.

[8] Z. Miao, T. Baležentis, S. Shao, and D. Chang, "Energy use, industrial soot and vehicle exhaust pollution—China's regional air pollution recognition, performance decomposition and governance," *Energy Economics*, vol. 83, pp. 501–514, 2019.

[9] H. Yang, M. Ma, J. R. Thompson, and R. J. Flower, "Waste management, informal recycling, environmental pollution and public health.," *Journal of epidemiology and community health*, vol. 72, no. 3, pp. 237–243, Mar. 2018.

[10] J. Wang *et al.*, "Vehicle emission and atmospheric pollution in China: problems, progress, and prospects," *PeerJ*, vol. 7, p. e6932, May 2019.

[11] T. Wang and S. Xie, "Assessment of traffic-related air pollution in the urban streets before and during the 2008 Beijing Olympic Games traffic control period," *Atmospheric Environment*, vol. 43, no. 35, pp. 5682–5690, 2009.

[12] Lynette W. Cheah, "Cars on a Diet: The Material and Energy Impacts of Passenger Vehicle Weight Reduction in the U.S," *Ph.D. Thesis - Massachusetts Institute of Technology, Engineering Systems Division*, 2010.

[13] Z. Mohamed-Kassim and A. Filippone, "Fuel savings on a heavy vehicle via aerodynamic drag reduction," *Transportation Research Part D: Transport and Environment*, vol. 15, no. 5, pp. 275–284, 2010.

[14] R. Vitolo and S. d'Ambrosio, "Potential impact of active tire pressure management on fuel consumption reduction in passenger vehicles," *Proceedings of the Institution of Mechanical Engineers Part D Journal of Automobile Engineering*, Mar. 2018.

[15] H. Aldhufairi and O. Olatunbosun, "Developments in tyre design for lower rolling resistance: a state of the art review," *Proceedings of the Institution of Mechanical Engineers, Part D: Journal of Automobile Engineering*, p. 095440701772719, Nov. 2017.

[16] M. Goharimanesh, A. Akbari, and A. Akbarzadeh Tootoonchi, "More efficiency in fuel consumption using gearbox optimization based on Taguchi method," *Journal of Industrial Engineering International*, vol. 10, no. 2, p. 61, 2014.

[17] S. F. Silva, E. M. Fernandes, and W. F. Amorim Junior, "Simulation-Driven Model-Based Approach for the Performance and Fuel Efficiency Trade-Off Evaluation of Vehicle Powertrain." SAE International, 2019.

[18] J. W. G. Turner *et al.*, "Ultra Boost for Economy: Extending the Limits of Extreme Engine Downsizing," *SAE Int. J. Engines*, vol. 7, no. 1, pp. 387–417, 2014.

[19] J. J. Eckert, F. M. Santiciolli, R. Yamashita, F. C. Corrêa, L. C. A. Silva, and F. G. Dedini, "Fuzzy Gear Shifting Control Optimization to Improve Vehicle Performance, Fuel Consumption and Engine Emissions," *IET Control Theory & Applications*, vol. 13, no. 16, pp. 2658–2669, 2019.

[20] J. J. Eckert, F. C. Corrêa, F. M. Santiciolli, E. D. S. Costa, H. J. Dionísio, and F. G. Dedini, "Vehicle gear shifting strategy optimization with respect to performance and fuel consumption," *Mechanics Based Design of Structures and Machines*, vol. 44, no. 1–2, pp. 123–136, 2016.

[21] T. P. Barbosa, J. J. Eckert, L. C. A. Silva, L. A. R. da Silva, J. C. H. Gutiérrez, and F. G. Dedini, "Gear shifting optimization applied to a flex-fuel vehicle under real driving conditions," *Mechanics Based Design of Structures and Machines*, pp. 1–18, 2020.

[22] J. Eckert, F. Santiciolli, L. Silva, F. Corrêa, and F. Dedini, "Design of an Aftermarket Hybridization Kit: Reducing Costs and Emissions Considering a Local Driving Cycle," vol. 1, pp. 210–235, Mar. 2020.

[23] J. J. Eckert, L. C. de A. e Silva, E. dos S. Costa, F.

M. Santiciolli, F. C. Corrêa, and F. G. Dedini, "Optimization of electric propulsion system for a hybridized vehicle," *Mechanics Based Design of Structures and Machines*, vol. 47, no. 2, pp. 175–200, Mar. 2019.

[24] I. Shancita, H. H. Masjuki, M. A. Kalam, I. M. Rizwanul Fattah, M. M. Rashed, and H. K. Rashedul, "A review on idling reduction strategies to improve fuel economy and reduce exhaust emissions of transport vehicles," *Energy Conversion and Management*, vol. 88, pp. 794–807, 2014.

[25] M. Furushou, K. Nishizawa, T. Iwasaki, and M. Tahara, "Stop-Start System with Compact Motor Generator and Newly Developed Direct Injection Gasoline Engine," Apr. 2012.

[26] Green Car Congress, "Ford concentrates on control strategies for low-cost start-stop system for Fusion." .

[27] S. Hawkins *et al.*, "Development of General Motors' eAssist Powertrain," *SAE International Journal of Alternative Powertrains*, vol. 1, pp. 308–323, Jul. 2012.

[28] E. Wiedemann, M. Karl, C. Ebner, and A. Sonntag, "From the environmental model to the intelligent engine stop start system," *18. Internationales Stuttgarter Symposium, Springer Fachmedien Wiesbaden*, pp. 165–178, 2018.

[29] Robin Rockström, "An engine start/stop strategy for a hybrid city bus," *Master of Science Thesis, KTH Industrial Engineering and Management*, 2009.

[30] M. V. Palwe and P. Kanjalkar, "Development and validation of enginestart/stop strategy for p2 hybrid electric vehicle," *Inventive Computation Technologies, Springer Interna-tional Publishing*, pp. 59–66, 2020.

[31] J. Bishop, A. Nedungadi, G. Ostrowski, B. Surampudi, P. Armiroli, and E. Taspinar, *An Engine Start/Stop System for Improved Fuel Economy*. 2007.

[32] J. Wishart, M. Shirk, T. Gray, and N. Fengler, "Quantifying the Effects of Idle-Stop Systems on Fuel Economy in Light-Duty Passenger Vehicles," *SAE 2012 World Congress & Exhibition*, Apr. 2012.

[33] N. Fonseca, J. Casanova, and M. Valdés, "Influence of the stop/start system on CO2 emissions of a diesel vehicle in urban traffic," *Transportation Research Part D: Transport and Environment*, vol. 16, no. 2, pp. 194–200, 2011.

[34] L. A. DeBruin, "Energy and Feasibility Analysis of Gasoline Engine Start/Stop Technology," *B.S. Thesis, Ohio State University*, 2013.

[35] L. Gaines, E. Rask, and G. Keller, "Which Is Greener: Idle, or Stop and Restart? Comparing Fuel Use and Emissions for Short Passenger-Car Stops," *Argonne National Laboratory*, 2013.

[36] M. Matsuura, K. Korematsu, and J. Tanaka, "Fuel Consumption Improvement of Vehicles by Idling Stop." SAE International , 2004.

[37] Q. Zhong, H. Qin, and R. Xu, "Study on the Start-Stop System Control Strategy under Different Driving Cycle," in *2018 IEEE 14th International Conference on Control and Automation (ICCA)*, 2018, pp. 223–228.

[38] T. D. Gillespie, "Fundamentals of vehicle dynamics," SAE Technical Paper, 1992.

[39] G. J. L. Naus, M. A. Beenakkers, R. G. M. Huisman, M. J. G. van de Molengraft, and M. Steinbuch, "Robust control of a clutch system to prevent judder-induced driveline oscillations," *Vehicle System Dynamics*, vol. 48, no. 11, pp. 1379–1394, Nov. 2010.

[40] M. Kulkarni, T. Shim, and Y. Zhang, "Shift dynamics and control of dual-clutch transmissions," *Mechanism and Machine Theory*, vol. 42, no. 2, pp. 168–182, 2007.

[41] R. N. Jazar, *Vehicle Dynamics: Theory and Application*. Springer New York, 2013.

[42] General Motors Brazil Ltda, "Owner Manual Chevrolet Celta 2013," 2013.

[43] B. Kramer *et al.*, "ADVISOR: a systems analysis tool for advanced vehicle modeling," *Journal of Power Sources*, vol. 110, no. 2, pp. 255–266, 2002.

[44] M. L. M. Oliveira, C. M. Silva, R. Moreno-Tost, T. L. Farias, A. Jiménez-López, and E. Rodríguez-Castellón, "Modelling of NOx emission factors from heavy and light-duty vehicles equipped with advanced aftertreatment systems," *Energy Conversion and Management*, vol. 52, no. 8, pp. 2945–2951, 2011.

[45] J. Eckert, F. Santiciolli, R. Yamashita, F. Correa, L. C. A. Silva, and F. Dedini, "Fuzzy Gear Shifting Control Optimization to Improve Vehicle Performance, Fuel Consumption and Engine Emissions," *IET Control Theory & Applications*, Aug. 2019.

[46] J. J. Eckert, F. M. Santiciolli, L. C. A. Silva, and F. G. Dedini, "Vehicle drivetrain design multi-objective optimization," *Mechanism and Machine Theory*, vol. 156, 2021.

[47] J. D. K. Bishop, M. E. J. Stettler, N. Molden, and A. M. Boies, "Engine maps of fuel use and emissions from transient driving cycles," *Applied Energy*, vol. 183, pp. 202–217, 2016.

[48] J. J. Eckert *et al.*, "Gear shifting multi-objective optimization to improve vehicle performance, fuel consumption, and engine emissions," *Mechanics Based Design of Structures and Machines*, vol. 46, no. 2, 2018.

[49] NBR 6601, "Light road motor vehicles - Determination of hydrocarbons, carbon monoxide, nitrogen oxides, carbon dioxides and particulate matter in the exhaust gas.," *ABNT*, 2012.

[50] A. M. Oliveira *et al.*, "Evaluation of Energy Recovery Potential through Regenerative Braking for a Hybrid Electric Vehicle in a Real Urban Drive Scenario." SAE International, 2016.

[51] J. J. Eckert *et al.*, "Fuel consumption and emissions analysis for a hybridized vehicle," in *Anais do XXIV Simpósio Internacional de Engenharia Automotiva*, 2016.